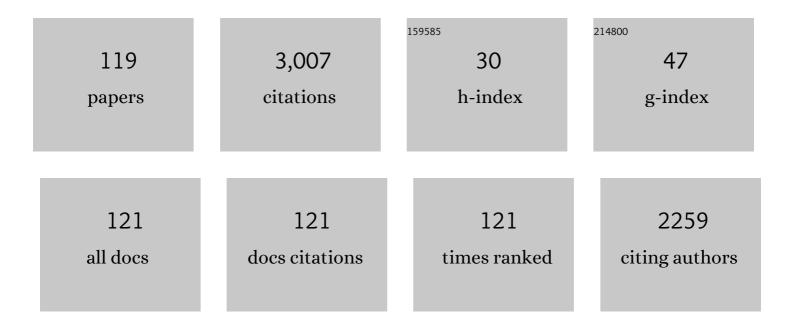
List of Publications by Year in descending order

Source: https://exaly.com/author-pdf/2120800/publications.pdf Version: 2024-02-01



SONA PARISSI

#	Article	IF	CITATIONS
1	Aqueous mixture viscosities of phenolic deep eutectic solvents. Fluid Phase Equilibria, 2022, 553, 113290.	2.5	4
2	A comprehensive experimental and modeling study on CO2 solubilities in the deep eutectic solvent based on choline chloride and butane-1,2-diol. Fluid Phase Equilibria, 2022, 561, 113535.	2.5	6
3	A global transform for the general formulation of liquid viscosities with significant linearizing benefits: a case study on ionic liquid mixtures. Physical Chemistry Chemical Physics, 2021, 23, 22551-22566.	2.8	5
4	Group contribution and atomic contribution models for the prediction of various physical properties of deep eutectic solvents. Scientific Reports, 2021, 11, 6684.	3.3	24
5	Experimental investigation of carbon dioxide solubility in the deep eutectic solvent (1 ChClÂ+Â3) Tj ETQq1 1 0.78	84314 rgB1 4.9	「/Overlock
6	Extension of SAFT-Î ³ to model the phase behavior of CO2+ionic liquid systems. Fluid Phase Equilibria, 2021, 538, 113026.	2.5	2
7	Volumetric investigation of aqueous mixtures of the {choline chlorideÂ+Âphenol (1:4)} deep eutectic solvent. Journal of Chemical Thermodynamics, 2021, 158, 106440.	2.0	9
8	Viscosity Investigations on the Binary Systems of (1 ChCl:2 Ethylene Glycol) DES and Methanol or Ethanol. Molecules, 2021, 26, 5513.	3.8	10
9	Determination of the Solute Content and Volumetric Properties of Binary Ionic Liquid Mixtures Using a Global Regularity of Molar Volume Expansion. Industrial & Engineering Chemistry Research, 2021, 60, 15274-15288.	3.7	0
10	Simple estimations of the speed of sound in ionic liquids, with and without any physical property data available. Fluid Phase Equilibria, 2020, 503, 112291.	2.5	7
11	Cobalt-molybdenum catalysts for the hydrodeoxygenation of cyclohexanone. Renewable Energy, 2020, 150, 443-455.	8.9	29
12	A novel atomic contribution model for the standard chemical exergies of organic compounds. Fluid Phase Equilibria, 2020, 507, 112397.	2.5	11
13	Experimental Measurement and Thermodynamic Modeling of Methane Solubility in Triethylene Glycol within the Temperature Range of 343.16–444.95 K. Journal of Chemical & Engineering Data, 2020, 65, 3866-3874.	1.9	8
14	Experimental measurements and thermodynamic modeling of high-pressure propane solubility in triethylene glycol. Journal of Supercritical Fluids, 2020, 163, 104881.	3.2	7
15	Estimation of the critical properties of compounds using volumeâ€based thermodynamics. AICHE Journal, 2020, 66, e17004.	3.6	6
16	A simple model for the viscosities of deep eutectic solvents. Fluid Phase Equilibria, 2020, 521, 112662.	2.5	44
17	A study of non-ideal mixtures of ethanol and the (1 choline chloride +2 ethylene glycol) deep eutectic solvent for their volumetric behaviour. Journal of Chemical Thermodynamics, 2020, 150, 106219.	2.0	15
18	Experimental investigation on the volumetric properties of mixtures of the deep eutectic solvent of Ethaline and methanol in the temperature range of 283.15 to 323.15â€K. Journal of Chemical Thermodynamics, 2020, 147, 106124.	2.0	17

#	Article	IF	CITATIONS
19	Experimental study and thermodynamic modeling of CCl4Â+ O2 and CCl4Â+ N2 hydrate equilibria. Fluid Phase Equilibria, 2020, 514, 112571.	2.5	3
20	A general model for the surface tensions of deep eutectic solvents. Journal of Molecular Liquids, 2020, 307, 112972.	4.9	30
21	Generalized Model to Estimate the Refractive Indices of Deep Eutectic Solvents. Journal of Chemical & Engineering Data, 2020, 65, 3965-3976.	1.9	14
22	Experimental investigation and thermodynamic modeling of xenon clathrate hydrate stability conditions. Fluid Phase Equilibria, 2020, 512, 112528.	2.5	11
23	The utilization of synthesis gas for the deoxygenation of cyclohexanone over aluminaâ€supported catalysts: Screening catalysts. Asia-Pacific Journal of Chemical Engineering, 2020, 15, e2425.	1.5	11
24	Upgrading of cyclohexanone to hydrocarbons by hydrodeoxygenation over nickel–molybdenum catalysts. International Journal of Hydrogen Energy, 2020, 45, 11062-11076.	7.1	28
25	Investigating the performance of novel green solvents in absorption refrigeration cycles: Energy and exergy analyses. International Journal of Refrigeration, 2020, 113, 174-186.	3.4	24
26	Energy Conservation in Absorption Refrigeration Cycles Using DES as a New Generation of Green Absorbents. Entropy, 2020, 22, 409.	2.2	14
27	A Clobal Model for the Estimation of Speeds of Sound in Deep Eutectic Solvents. Molecules, 2020, 25, 1626.	3.8	8
28	Estimation of the heat capacities of deep eutectic solvents. Journal of Molecular Liquids, 2020, 307, 112940.	4.9	29
29	Estimation of viscosities of 1-alkyl-3-methylimidazolium ionic liquids over a range of temperatures using a simple correlation. Physics and Chemistry of Liquids, 2019, 57, 401-421.	1.2	7
30	Experimental Investigation of Liquid–Liquid Extraction of Toluene + Heptane or Toluene + Hexane Using Deep Eutectic Solvents. Journal of Chemical & Engineering Data, 2019, 64, 3811-3820.	1.9	23
31	Simple and global correlation for the densities of deep eutectic solvents. Journal of Molecular Liquids, 2019, 296, 111830.	4.9	42
32	A Theoretical and Experimental Study for Screening Inhibitors for Styrene Polymerization. Processes, 2019, 7, 677.	2.8	11
33	Deep eutectic solvents for CO2 capture from natural gas by energy and exergy analyses. Journal of Environmental Chemical Engineering, 2019, 7, 103411.	6.7	25
34	Experimental investigation of acid regeneration of spent bleaching clay de-oiled by the in-situ transesterification process at various operating conditions. Chemical Engineering Research and Design, 2019, 124, 121-127.	5.6	11
35	Post-discharge DBD plasma treatment for degradation of organic dye in water: A comparison with different plasma operation methods. Journal of Environmental Chemical Engineering, 2019, 7, 103220.	6.7	32
36	Densities and volumetric properties of (choline chloride + urea) deep eutectic solvent and methanol mixtures in the temperature range of 293.15–323.15â€⊤K. Journal of Chemical Thermodynamics, 2018, 124, 10-20.	2.0	59

#	Article	IF	CITATIONS
37	Experimental study on the effects of an ionic liquid for CO2 capture using hollow fiber membrane contactors. International Journal of Greenhouse Gas Control, 2018, 69, 1-7.	4.6	33
38	Modeling the Phase Behavior of Carbon Dioxide Solubility in Deep Eutectic Solvents with the Cubic Plus Association Equation of State. Journal of Chemical & Engineering Data, 2018, 63, 897-906.	1.9	33
39	A general viscosity model for deep eutectic solvents: The free volume theory coupled with association equations of state. Fluid Phase Equilibria, 2018, 470, 193-202.	2.5	83
40	Modeling vapor-liquid equilibria of mixtures of SO2 and deep eutectic solvents using the CPA-NRTL and CPA-UNIQUAC models. Journal of Molecular Liquids, 2018, 250, 259-268.	4.9	28
41	The friction theory for modeling the viscosities of deep eutectic solvents using the CPA and PC-SAFT equations of state. Journal of Molecular Liquids, 2018, 249, 554-561.	4.9	40
42	Excess volumes of mixtures consisting of deep eutectic solvents by the Prigogine–Flory–Patterson theory. Journal of Molecular Liquids, 2018, 272, 731-737.	4.9	10
43	The Biodiesel of Microalgae as a Solution for Diesel Demand in Iran. Energies, 2018, 11, 950.	3.1	19
44	Investigation of solutions of ethyl alcohol and the deep eutectic solvent of Reline for their volumetric properties. Fluid Phase Equilibria, 2018, 472, 39-47.	2.5	38
45	Bridging the Generation Gap in Scientific Writing—New Flexibility in Reference Formats. Journal of Chemical & Engineering Data, 2018, 63, 1849-1850.	1.9	1
46	Prediction of the surface tension of binary liquid mixtures of associating compounds using the Cubic Plus Association (CPA) equation of state. Journal of Molecular Liquids, 2017, 231, 451-461.	4.9	10
47	Recovery of volatile fatty acids from water using medium-chain fatty acids and a cosolvent. Chemical Engineering Science, 2017, 165, 74-80.	3.8	28
48	Estimation of viscosities of pure ionic liquids using an artificial neural network based on only structural characteristics. Journal of Molecular Liquids, 2017, 227, 309-317.	4.9	30
49	A novel correlative approach for ionic liquid thermal conductivities. Journal of Molecular Liquids, 2017, 236, 214-219.	4.9	18
50	Investigation of propane addition to the feed stream of a commercial ethane thermal cracker as supplementary feedstock. Journal of the Taiwan Institute of Chemical Engineers, 2017, 81, 1-13.	5.3	13
51	Experimental investigation on CO 2 absorption in Sulfinol-M based Fe 3 O 4 and MWCNT nanofluids. International Journal of Refrigeration, 2017, 73, 1-10.	3.4	59
52	Vapor–Liquid Equilibria of Binary and Ternary Mixtures of Acetaldehyde with Versatic 9 and Veova 9. Journal of Chemical & Engineering Data, 2016, 61, 2114-2119.	1.9	3
53	Estimation of the Densities of Ionic Liquids Using a Group Contribution Method. Journal of Chemical & Engineering Data, 2016, 61, 4031-4038.	1.9	22
54	A new Peng-Robinson modification to enhance dew point estimations of natural gases. Journal of Natural Gas Science and Engineering, 2016, 34, 1137-1147.	4.4	18

#	Article	IF	CITATIONS
55	A new configuration in the tail-end acetylene hydrogenation reactor to enhance catalyst lifetime and performance. Journal of the Taiwan Institute of Chemical Engineers, 2016, 65, 8-21.	5.3	6
56	Modeling gas solubilities in imidazolium based ionic liquids with the [Tf 2 N] anion using the GC-EoS. Fluid Phase Equilibria, 2016, 409, 408-416.	2.5	13
57	Upgrading Process of 4-Methylanisole as a Lignin-Derived Bio-Oil Catalyzed by Pt/l³-Al ₂ O ₃ : Kinetic Investigation and Reaction Network Development. Energy & Fuels, 2015, 29, 3335-3344.	5.1	36
58	Solubility of Carbon Dioxide in Secondary Butyl Alcohol at High Pressures: Experimental and Modeling with CPA. Journal of Solution Chemistry, 2015, 44, 1555-1567.	1.2	5
59	Upgrading of Lignin-Derived Bio-oil Components Catalyzed by Pt/γ-Al ₂ O ₃ : Kinetics and Reaction Pathways Characterizing Conversion of Cyclohexanone with H ₂ . Energy & Fuels, 2015, 29, 191-199.	5.1	41
60	A simple group contribution correlation for the prediction of ionic liquid heat capacities at different temperatures. Fluid Phase Equilibria, 2015, 403, 95-103.	2.5	53
61	Kinetics of Upgrading of Anisole with Hydrogen Catalyzed by Platinum Supported on Alumina. Energy & Fuels, 2015, 29, 4990-4997.	5.1	44
62	Experimental investigation of ionic liquid pretreatment of sugarcane bagasse with 1,3-dimethylimadazolium dimethyl phosphate. Bioresource Technology, 2015, 185, 411-415.	9.6	31
63	Modeling of ionic liquid+polar solvent mixture molar volumes using a generalized volume translation on the Peng–Robinson equation of state. Fluid Phase Equilibria, 2015, 395, 51-57.	2.5	30
64	Two simple correlations to predict viscosities of pure and aqueous solutions of ionic liquids. Journal of Molecular Liquids, 2015, 211, 948-956.	4.9	20
65	Investigation of volumetric fluid properties of (heptaneÂ+Âhexadecane) at reservoir conditions. Journal of Natural Gas Science and Engineering, 2015, 22, 377-394.	4.4	7
66	Conversion enhancement of heavy reformates into xylenes by optimal design of a novel radial flow packed bed reactor, applying a detailed kinetic model. Chemical Engineering Research and Design, 2015, 95, 317-336.	5.6	10
67	Investigating the efficiency of MEOR processes using Enterobacter cloacae and Bacillus stearothermophilus SUCPM#14 (biosurfactant-producing strains) in carbonated reservoirs. Journal of Petroleum Science and Engineering, 2014, 113, 46-53.	4.2	52
68	Estimation of viscosity of binary mixtures of ionic liquids and solvents using an artificial neural network based on the structure groups of the ionic liquid. Fluid Phase Equilibria, 2014, 364, 88-94.	2.5	32
69	Derivative Properties from High-Precision Equations of State. Journal of Physical Chemistry B, 2014, 118, 14397-14409.	2.6	9
70	Vapor–Liquid Equilibria of the Binary System 1,5-Hexadiene + Allyl Chloride. Journal of Chemical & Engineering Data, 2014, 59, 52-55.	1.9	1
71	An artificial neural network to calculate pure ionic liquid densities without the need for any experimental data. Journal of Supercritical Fluids, 2014, 95, 60-67.	3.2	26
72	Bubble-point pressures of binary and ternary mixtures of acetaldehyde with Versatic 10 and Veova 10. Fluid Phase Equilibria, 2014, 368, 1-4.	2.5	3

#	Article	IF	CITATIONS
73	Support vector machine and CPA EoS for the prediction of high-pressure liquid densities of normal alkanols. Journal of the Taiwan Institute of Chemical Engineers, 2014, 45, 2888-2898.	5.3	7
74	High pressure phase behavior of methanol+ethylene: Experimental measurements and CPA modeling. Journal of Supercritical Fluids, 2014, 92, 47-54.	3.2	3
75	Biodiesel Production from High Free Fatty Acid-Content Oils: Experimental Investigation of the Pretreatment Step. APCBEE Procedia, 2013, 5, 474-478.	0.5	53
76	Vapor–liquid equilibria of isopropyl alcohol+propylene at high pressures: Experimental measurement and modeling with the CPA EoS. Journal of Supercritical Fluids, 2013, 84, 182-189.	3.2	14
77	Vapor-liquid equilibria of binary mixtures of propylene oxide with either ethyl benzene, 2-methylpentane, or 2-methyl-1-pentene. Fluid Phase Equilibria, 2013, 352, 97-99.	2.5	2
78	High pressure phase behaviour of mixtures of hydrogen and the ionic liquid family [cnmim][Tf2N]. Journal of Supercritical Fluids, 2013, 73, 126-129.	3.2	19
79	Solubility of carbon monoxide in methyl methacrylate at high pressures. Journal of Supercritical Fluids, 2013, 73, 138-140.	3.2	1
80	Liquid–Liquid Equilibria in Biodiesel Production. JAOCS, Journal of the American Oil Chemists' Society, 2013, 90, 147-154.	1.9	22
81	Purification of flue gas by ionic liquids: Carbon monoxide capture in [bmim][Tf ₂ N]. AICHE Journal, 2013, 59, 3886-3891.	3.6	41
82	A simple correlation to predict high pressure solubility of carbon dioxide in 27 commonly used ionic liquids. Journal of Supercritical Fluids, 2013, 77, 158-166.	3.2	42
83	Correlating bubble points of ternary systems involving nine solvents and two ionic liquids using artificial neural network. Fluid Phase Equilibria, 2013, 352, 34-41.	2.5	21
84	Experimental investigation and modeling of liquid–liquid equilibria in two systems of concern in biodiesel production. Fluid Phase Equilibria, 2013, 353, 31-37.	2.5	10
85	PERCEPTRON ARTIFICIAL NEURAL NETWORK AND PREDICTION OF BUBBLE POINTS OF TERNARY MIXTURES CONTAINING IONIC LIQUIDS. Journal of Theoretical and Computational Chemistry, 2013, 12, 1350053.	1.8	2
86	Evaluation of maximum gasoline production of Fischer–Tropsch synthesis reactions in GTL technology: A discretized approach. Journal of Natural Gas Science and Engineering, 2012, 9, 209-219.	4.4	13
87	Liquid–Liquid Phase Equilibria of Systems of Palm and Soya Biodiesels: Experimental and Modeling. Industrial & Engineering Chemistry Research, 2012, 51, 8302-8307.	3.7	15
88	Estimation of Thermal Conductivity of Ionic Liquids Using a Perceptron Neural Network. Industrial & Engineering Chemistry Research, 2012, 51, 9886-9893.	3.7	85
89	Understanding temperature dependency of hydrogen solubility in ionic liquids, including experimental data in [bmim][Tf ₂ N]. AICHE Journal, 2012, 58, 3553-3559.	3.6	39
90	Using artificial neural network to predict the ternary electrical conductivity of ionic liquid systems. Fluid Phase Equilibria, 2012, 314, 128-133.	2.5	63

#	Article	IF	CITATIONS
91	High-pressure vapor–liquid equilibria of methanol+propylene: Experimental and modeling with SAFT. Journal of Supercritical Fluids, 2012, 63, 25-30.	3.2	7
92	Modeling gas solubility in ionic liquids with the SAFT-Î ³ group contribution method. Journal of Supercritical Fluids, 2012, 63, 81-91.	3.2	37
93	An IUPAC Task Group Study: The Solubility of Carbon Monoxide in [hmim][Tf ₂ N] at High Pressures. Journal of Chemical & Engineering Data, 2011, 56, 4797-4799.	1.9	16
94	Hydrogen Solubilities in the IUPAC Ionic Liquid 1-Hexyl-3-methylimidazolium Bis(Trifluoromethylsulfonyl)Imide. Journal of Chemical & Engineering Data, 2011, 56, 1105-1107.	1.9	37
95	Enhancement in Triethylene Glycol (TEG) Purity via Hydrocarbon Solvent Injection to a TEG + Water System in a Batch Distillation Column. Energy & Fuels, 2011, 25, 5126-5137.	5.1	21
96	Enhancement in NGL production and improvement in water dew point temperature by optimization of slug catchers' pressures in water dew point adjustment unit. Journal of Natural Gas Science and Engineering, 2011, 3, 326-333.	4.4	6
97	Considering multiple occupancy of cavities in clathrate hydrate phase equilibrium calculations. Journal of Chemical Thermodynamics, 2011, 43, 822-827.	2.0	8
98	High pressure phase behaviour of methane in 1-butyl-3-methylimidazolium bis(trifluoromethylsulfonyl)imide. Fluid Phase Equilibria, 2010, 294, 67-71.	2.5	79
99	Scott–van Konynenburg phase diagram of carbon dioxide+alkylimidazolium-based ionic liquids. Journal of Supercritical Fluids, 2010, 55, 825-832.	3.2	48
100	Carbon Dioxide Solubility in the Homologous 1-Alkyl-3-methylimidazolium Bis(trifluoromethylsulfonyl)imide Family. Journal of Chemical & Engineering Data, 2009, 54, 382-386.	1.9	129
101	A potential ionic liquid for CO ₂ -separating gas membranes: selection and gas solubility studies. Green Chemistry, 2009, 11, 185-192.	9.0	118
102	Ethane as an alternative solvent for supercritical extraction of orange peel oils. Journal of Supercritical Fluids, 2008, 45, 306-313.	3.2	49
103	High-Pressure Phase Behavior of Ethane with 1-Hexyl-3-methylimidazolium Bis(trifluoromethylsulfonyl)imide. Journal of Chemical & Engineering Data, 2008, 53, 1283-1285.	1.9	40
104	Solubility of carbon dioxide in the ionic liquid 1-ethyl-3-methylimidazolium bis(trifluoromethylsulfonyl)imide. Fluid Phase Equilibria, 2007, 260, 19-22.	2.5	166
105	Chapter 9. CO2 Solubility in Alkylimidazolium-Based Ionic Liquids. , 2007, , 131-149.		3
106	Application of double retrograde vaporization as an optimizing factor in supercritical fluid separations. Journal of Supercritical Fluids, 2005, 33, 115-120.	3.2	13
107	Liquid–vapor and liquid–liquid–vapor equilibria in the ternary system ethane+limonene+linalool. Journal of Supercritical Fluids, 2005, 33, 201-208.	3.2	13
108	Experimental determination of high-pressure phase equilibria of the ternary system carbon dioxide+limonene+linalool. Journal of Supercritical Fluids, 2005, 35, 10-17.	3.2	50

#	Article	IF	CITATIONS
109	Thermodynamic Analysis of the Phenomenon of Double Retrograde Vaporization. Journal of Physical Chemistry B, 2004, 108, 13771-13776.	2.6	6
110	High pressure phase behavior of the system ethane+orange peel oil. Journal of Supercritical Fluids, 2004, 29, 59-67.	3.2	13
111	Double retrograde vaporization in a multi-component system: ethane+orange peel oil. Journal of Supercritical Fluids, 2004, 29, 69-75.	3.2	12
112	Phase behaviour of the catalyst dicarbonyl(η5-cyclopentadienyl)-cobalt in carbon dioxide. Journal of Supercritical Fluids, 2004, 31, 1-8.	3.2	9
113	Prediction of double retrograde vaporization: transitions in binary mixtures of near critical fluids with components of homologous series. Journal of Supercritical Fluids, 2004, 32, 63-71.	3.2	10
114	Simulation of double retrograde vaporization using the Peng–Robinson equation of state. Journal of Chemical Thermodynamics, 2003, 35, 573-581.	2.0	19
115	Phase behaviour of the binary system ethane+limonene. Journal of Supercritical Fluids, 2002, 22, 93-102.	3.2	15
116	Double retrograde vaporization in the binary system ethane+linalool. Journal of Supercritical Fluids, 2002, 23, 1-9.	3.2	14
117	Phase behavior of the binary system ethane+linalool. Journal of Supercritical Fluids, 2002, 24, 111-121.	3.2	17
118	On the phenomenon of double retrograde vaporization: multi-dew point behavior in the binary system ethane + limonene. Fluid Phase Equilibria, 2001, 191, 33-40.	2.5	23
119	Bubble-point pressures of the binary system carbon dioxide+linalool. Journal of Supercritical Fluids, 2001, 20, 221-228.	3.2	74